AUN/SEED-Net JICA

# 8th AUN/SEED-Net
## REGIONAL CONFERENCE ON ELECTRICAL AND ELECTRONICS ENGINEERING

Envision, Enable, and Empower
Smarter and Resilient Societies

*co-located with*

# 11th ERDT Conference
## on Semiconductor and Electronics, Information and Communications Technology and Energy

**16-17 November 2015**
**Metro Manila, Philippines**

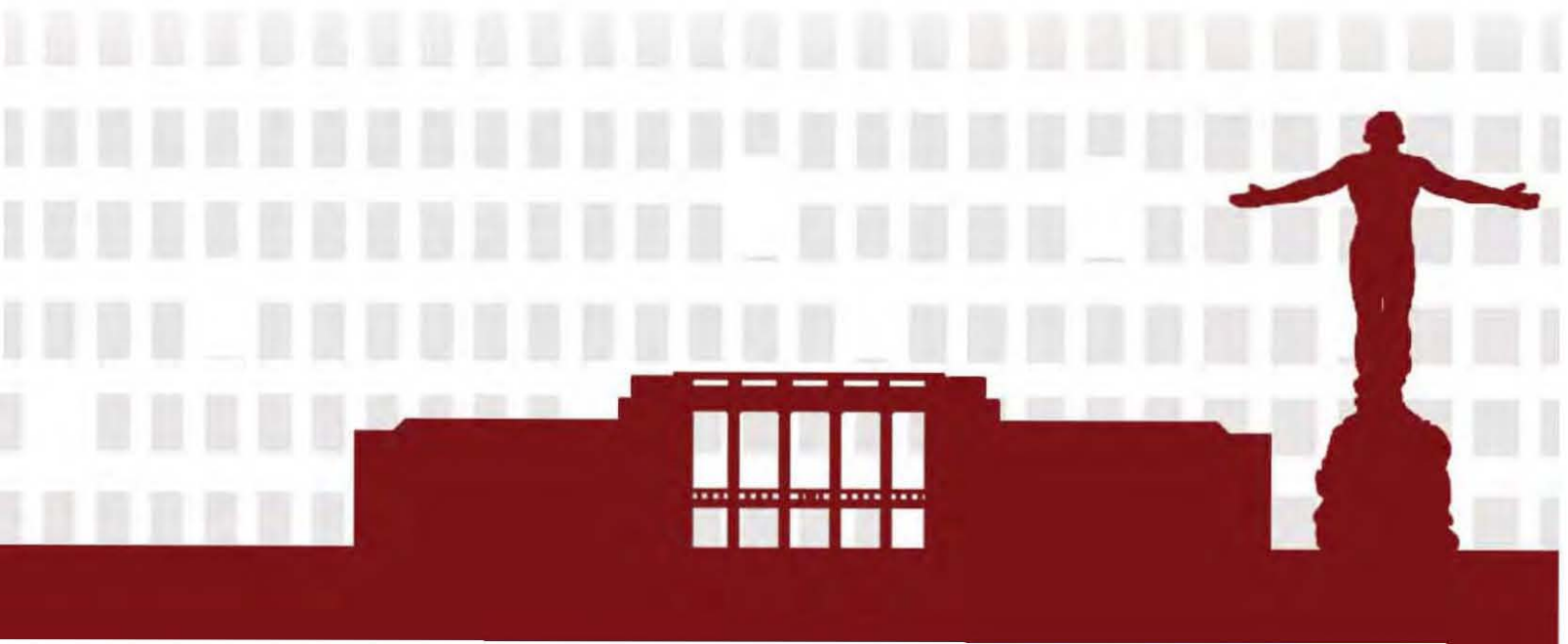

**Proceedings of the 8th AUN/SEED-Net RCEEE 2015 and 11th ERDT Conference**
**on Semiconductor and Electronics, Information and Communications Technology, and Energy**

Editors:
Dr. Joel Joseph S. Marciano Jr.
Dr. Jhoanna Rhodette I. Pedrasa
Dr. Rhandley D. Cajote



ISBN: 978-616-406-075-3

Published by: ASEAN University Network / Southeast Asia Engineering Education Development Network (AUN/SEED-Net) JICA Project
Faculty of Engineering, Bldg. 2
Chulalongkorn University, Bangkok
Thailand 10330

Printed in the Philippines by: ERZALAN PRINTING PRESS
45 Cotabato Street, Luzviminda Village, Batasan Hills, Quezon City, Philippines

# 8th AUN/SEED-Net Regional Conference
## on Electrical and Electronics Engineering 2015

co-located with

# 11th ERDT Conference
## on Semiconductor and Electronics, Information and Communications Technology, and Energy

# Envision, Enable and Empower Smarter and Resilient Societies

Published by: ASEAN University Network / Southeast Asia Engineering Education Development Network (AUN/SEED-Net) in partnership with Engineering Research and Development for Technology (ERDT) and University of the Philippines Diliman.


ISBN: 978-616-406-075-3

# DETECTION OF MICRO-CRACK DEFECT ON EGGSHEL BY MEANS OF CANDLE LIGHTING AND IMPROVED ANISTROPIC DIFFUSION FILTERING

**M. H. Abdullah and M. Z. Abdullah**

Electrical and Electronic Engineering, Universiti Sains Malaysia, Nibong Tebal, Pulau Pinang, MALAYSIA.
Email: mhaips10_eee1@student.usm.my, mza@usm.my

**Keywords:** Micro-crack Detection, Eggshell, Anisotropic Diffusion, Double Thresholding.

ABSTRACT
This paper investigates micro-crack detection on eggshell using computer vision technology. The highly textured image of the egg shell due the heterogeneity of its structure makes detection process a very challenging task. In order to enhance the micro-crack region and reduce anomalies, an improved thresholding equation incorporating the mean and gradient values of the image has been developed. The resulting image has been segmented using a double thresholding technique from which an edge image has been formed. The results have been qualitatively and quantitatively assessed from which it has been concluded that the proposed method achieved better performance in precision of FOM measure.

## 1. Introduction

In USA, 76.9 billion table eggs were processed yearly. Sorting, grading and packaging are three most commonly processes found in poultry production. With the advanced automation and online instrumentation, egg processing can now be performed at a very high-speed, reaching a rate exceeding 120,000 per hour in some cases (Lawrence et al., 2008). However, according to the Department of Agriculture (USDA), processed eggs still need to be manually checked in order to ensure the quality of the product. Approximately 4% of the processed eggs must be manually re-inspected in order to be compliant with USDA standard (Lawrence et al., 2008). Hence, human checking and manual inspection are integral parts in poultry farming (Yongyu, Sagar and Yankun, 2012).

One of the quality assessments performed during poultry processing is the inspection of micro-crack defect on eggshell. Since this defect is completely invisible to naked eyes, therefore, the inspection requires specialized instrmentation and computer hardware. Two most popular poultry inspection systems are: (i) the acoustic response (AR) and (ii) the computer vision (CV) (Pan et al., 2011). In AR inspection, the system utilizes a mechanical response induced by inflicting a light mechanical impact to the surface of eggshell. The cause of impact on intact and crack surfaces produces two different profiles of impulse responses (Wang and Jiang, 2005). In this approach, the right force for inflicting impacts on eggshells must be properly calibrated in order to ensure the physical integrity of eggs is preserved before and after inspection. The resulting responses are measured and analyzed electronically. The analyses are mostly performed in frequency domain and the details have been published elsewhere (Pan et al., 2011), (Wang and Jiang, 2005), (Sun et al., 2013). However, the AR response depends largely on few important physical characteristics of an egg especially the thickness and the size of the micro-crack (Wang and Jiang, 2005). These parameters need to be firstly measured in order to increase chances of detection and reduce false negative. The measurements are very time consuming and labor intensive work. Meanwhile a CV measurement usually requires a strong illuminator known as the candling light. In operation the illuminator is placed below the eggs, forming the back-lighting image capturing strategy. In this set-up the micro-crack will appear as white pixels because such a defect is fairly transparent to light. This method is proven to be very reliable in defect detection, resulting in a successful rate of consistently more than 90% (Lawrence et al., 2008), (Pan, Tu and Su, 2007). One advantage of CV is it is completely non-destructive and non-intrusive compared to the resonant technique. Besides, CV approach can process the detection faster than AR technique. The main difficulty with this technique is the image that it produces is very complicated because of the eggshell texture. The presence of other anomalies on the egg shell like scratches, dirts and grains results in very heterogeneous image and further complicates the detection process. Hence, the objective of this study is to develop the algorithm to enhance micro-crack pixels in CV image by filtering noise or unwanted components. The improved version of the anisotropic diffusion filter (ADF) is proposed for solving these problems. The results are compared with original ADF and its recent variants from which the conclusion is derived.

## 2. Materials And Methods

This section summarises the methods and procedures used in this work. The hardware of the machine inspector is first discussed, and followed with the software requirements, especially image filtering and binarisation.

### 2.1 Micro-crack System

The elements of the CV based egg inspection system include the high resolution camera, the color frame grabber board (CFGB) and the candling light source.

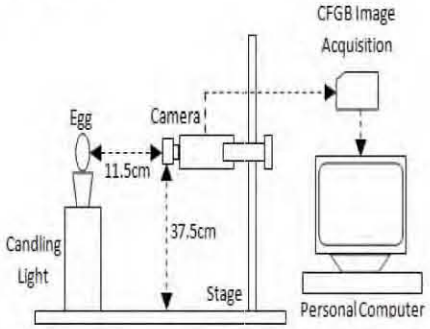


**Figure 1.** CV system for micro-crack detection of eggshell.

Figure 1 shows the set-up. The CFGB is manufactured by Matrox Electronic System Limited, Canada. For image capturing, a 3-CCD Sony XC- 003P camera with resolution of pixels is employed. Meanwhile a candling light comprising of 38 W halogen lamp manufactured by The Schlueter Company, Wisconsin, USA is used as an illuminator. As shown in Figure 1, the camera is mounted at a height of 37.5 cm and positioned approximately 11.5 cm from the target. This set-up enabled an optimally focused image be captured. Image capturing is performed in dark room in order to minimize inteference from the background.

### 2.2 Egg Samples

Altogether thirty fresh eggs were acquired from the poultry farm. The samples ranged from one to two days old. Each sample was imaged manually by trained human inspectors. Figure 2 shows example of micro-crack image of an eggshell obtained from a defected sample. It can be seen from Figure 2(a) that this defect appears like a hairline white-pixels with random pattern. As a comparison, Figure 2(b) shows an image of the same sample captured without a candling light. Clearly, the micro-crack defect is completely invisible to naked eyes in this image. Hence the reason why such a defect is referred to as the micro-crack defect in poultry farming.

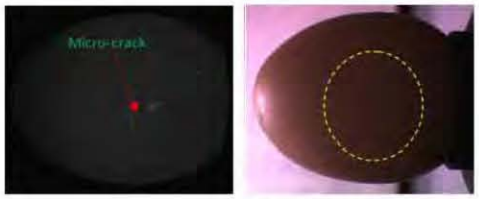


**Figure 2.** Example of an eggshell image with micro-crack captured using (a) candling light, (b) normal frontlighting. The dotted circle in (b) marks the area in which the micro-crack pixels are located.

### 2.3 Micro-crack Characteristic

Detection of micro-crack in eggshell using computer vision is a quite challenging because of the egg-shell is highly textured image as evident in Figure 2(a). There are various factors which contribute to textural complexities of the eggshell image. Among them is the inhomogeneity of the eggshell resulting in the appearance of small but randomly located white spots as clearly shown in this figure. The presence of anomalies like scratches and dirts further complicate the problem. Nevertheless the microcrack has very unique characteristics compared to other background anomalies. In order to highlight these characteristics, a horizontal line profile is drawn across an area containing micro-crack pixels. The results are shown in Figure 3. Clearly from this figure micro-crack defect is characterized by pixels having relatively high intensity and high gradient values. These properties are exploited in developing an algorithm for this type of defect detection.

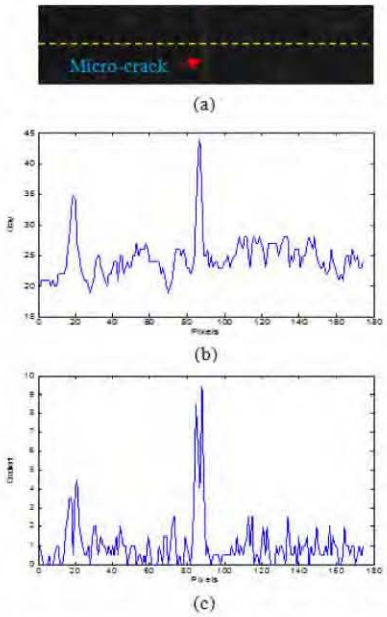


**Figure 3.** (a) The horizontal line is drawn across an area containing micro-crack pixels in Figure 2(a), (b) gray level profile of (a) and (c) gradient of (b).

### 2.4 Anisotropic Diffusion Filtering

The first step in the detection algorithm is to identify all pixels belonging to micro-crack defect. Based on previously mentioned characteristics of micro-crack pixels in that their intensities and gradients are relatively higher than the homogeneous background, therefore, the anisotropic diffusion filter (ADF) is found to be the most suitable algorithm for this application. The purpose of this filtering strategy is to produce a smoothed image with significant edges. This filter was first introduced by (Perona and Malik, 1990) in attempting to accurately binarise gray-level images acquired under non-uniform illumination. Since then there are several different types of ADF variants exist in the literatures. Here we only consider three ADF variants including the original ADF proposed by (Perona and Malik, 1990) before proposing our own ADF formula. They are briefly discussed below. The ADF generally describes a diffused image at iteration *t*. Mathematically,

$$I_d(x,y,t) = I_d(x,y,t-1) + \frac{1}{4}\sum_{i=1}^{4} c\left(\left|\nabla I_d^i\right|\right)\nabla I_d^i, t > 0 \qquad (1)$$

where $\nabla$ and $c$ are gradient and diffusion coefficients, respectively. The gradient of the image is calculated by using four Laplacian neighbour, $i = \{1,2,3,4\}$ referred to as north, south, east and west respectively. The diffusion coefficient proposed by the (Perona and Malik, 1990) can be written as follows:

$$c(s) = 1 + [1 + (\frac{s}{K})^2]^{-1} \qquad (2)$$

where $s = |\nabla I_d|$ . One of the main drawbacks of this diffusion equation is due to its sensitivity to noise, resulting in image blurring which in turn increasing the ambiguity between different regions of the image. A slight improvement to this problem is due to work by (Tsai, Chang and Choi, 2010) who proposed the modified equation as follows:

$$c(s) = 1 + [f(x,y) \cdot (\frac{K}{s})^2]^{-1} \qquad (3)$$

where $f(x,y)$ is normalized gray-leve and $K$ is a constant. In both (3) and (4), this parameter basically serves as edge strength threshold. This parameter must be properly selected in order to produce images with satisfactory quality. If $K$ is too small the diffusion process will terminate faster causing very little change in the output image. In contrary the output image will significantly be blurred if $K$ is too large. Both (Perona and Malik, 1990) and (Tsai, Chang and Choi, 2010) algorithm require parameter - to be fixed experimentally, often through trial-and-error method. Moreover the algorithm leads to local thresholding which is highly sensitive to illumination variation. In order to give a robust in noise and non-uniform illumination, few global versions of the (Perona and Malik, 1990) thresholding equation have been proposed. One of the recent variants is the result of the work by (Anwar and Abdullah, 2014). According to these authors, the diffusion coefficients needed in global thresholding can be computed as follows:

$$c(s) = 1 - [1 + (\frac{s}{g})^2]^{-1} \quad (4)$$

where $g$ is a mapping of the image intensity and calculated by using the sigmoid transfer function (Anwar and Abdullah, 2014). Unlike (2) and (3), equation (4) allows different threshold values to be selected based on local properties. A major advantage of this method is the significantly less influence of image noise since the thresholding is performed at low resolution in which the noise is suppressed. In order to further improve (4), this work proposes a new global approach to optimally separate the foreground and background so that white and black pixels can be correctly classified as many as possible. The proposed diffusion equation is given below:

$$c(s) = 1 + [1 + (\frac{s}{((g-\mu)/a)})^2]^{-1} \quad (5)$$

where $g$ is a mapping of the input image intensity, μ is a mean value of $g$ and 2 is a constant which needs to be determined heuristically. In (5), the combination of /and μ parameters are used to minimize problems associated with incomplete or missing edges which is quite prominent in (3) and (4). Instead of using one stopping threshold value for the whole pixels as in (2) and (3), our method uses the $g$ and μ parameters to generate the stopping threshold for each pixel. In this way, the proposed method would lead to an effective denoising, and hence, more accurate reconstruction of edge image.

### 2.5 Image Segmentation

In many pattern recognition applications, it is extremely important for object of interest be accurately segmented, so that noise or unwanted pixels could be reduced or altogether eliminated. In this study, a double thresholding technique is applied to reconstruct the binary image from diffused micro-crack pixels. The details of the double thresholding technique are presented in (Nashat, Abdullah and Abdullah, 2012). Using this technique the image is segmented using the Niblack dynamic method, and the threshold value can be calculated as follows:

$$\tau = \mu - \alpha\sigma \quad (6)$$

where $a$ is a scaling factor, 4 is the mean value and 6 is the standard deviation value. Both are calculated dynamically using the output image after filtering process. Generally, the double thresholding technique requires two sets of binary images to be analyzed. The first image is referred to as the target image 789 and the second image is known as the seed image 7:9 . Basically, this method requires an image to be segmented twice using high and low threshold values. In order to obtain these images, two scaling factors are used. The first one 5:9 calculates a seed image and the second one 589 calculates the target image as shown in (7) and (8). The idea of using two scaling factors is to generate two binary images. A seed image produces a set of image contains largely incomplete but almost noise-free edges and the target image contains complete edges including noises.

$$B_{SI} = \mu - \alpha_{SI}\sigma \quad (7)$$

$$B_{TI} = \mu - \alpha_{TI}\sigma \quad (8)$$

The edges are firstly reconstructed using outputs from (7) and (8). Second it is post processed using morphological operation and, finally followed by dilation and closing (Nashat, Abdullah and Abdullah, 2012). The flowchart in Figure 4 summarizes the overall procedure of the micro-crack detection of eggshell.

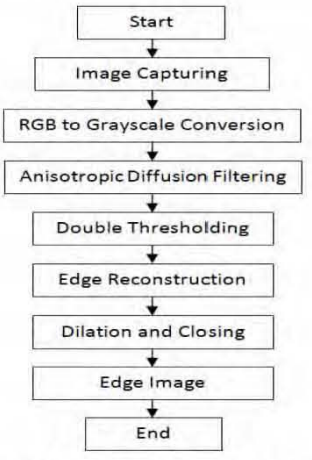


**Figure 4.** An algorithm for micro-crack detection of eggshell

## 3 Results And Discussion

### 3.1 Image Diffusion

The methods and procedures discussed previously are implemented on a personal computer equipped with Intel core 2 quad processor 2.5GHz and 1.96 GB of RAM. Experiments are performed using twenty egg samples containing micro-crack defects. In all cases the image is diffused 15 times, i.e. ; Example of diffused image obtained using (5) is displayed in Figure 5. This image was produced using Figure 2(a) as an input.

**Figure 5.** Example of diffused image using the proposed diffusion equation corresponding to an input image in Figure 2(a).

### 3.2 Image Segmentation

This section presents the result of image segmentation. Example of binary image produced by the proposed ADF equation is shown in Figure 6. In this case, Figures 6(a), 6(b) and 6(c) are seed, target and output images respectively. Clearly in Figure 6(c) the reconstructed image is very noisy since it contains many unwanted components or isolated pixels. Morphological operations are used to remove the unwanted pixels and clean-up speckle noise or the ghost artifacts. The result is shown in Figure 7. In this figure, the result is also visually compared with the original ADF formula and its recent variants. As can be seen from Figure 7, the unwanted connected binary components have effectively been removed in all cases.

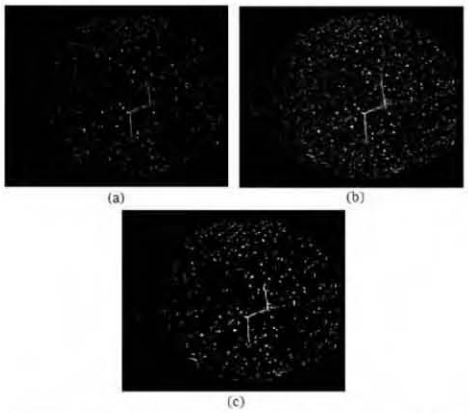


**Figure 6:** Segmentation results of Figure 5, (a) the seed image, (b) the target image, and (c) the reconstructed Image

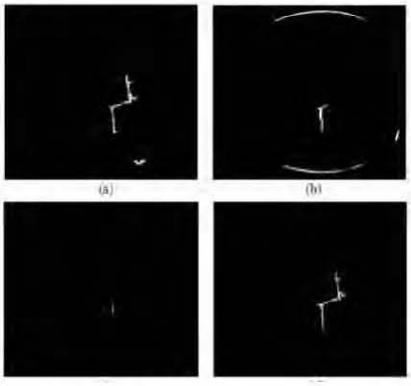

**Figure 7:** Binarisation results comparing (a) (Perona and Malik, 1990), (b) (Tsai, Chang and Choi, 2010), (c) (Anwar and Abdullah, 2014), and (d) proposed ADF algorithms.

In this example, the parameter $K$ was rigidly set to 4 in both (Perona and Malik, 1990) and (Tsai, Chang and Choi, 2010) diffusion equations. This value was determined through trial-and-error method and it was the best value for both algorithms. Close observation of Figures 7(a) and 7(b) revealed that the (Perona and Malik, 1990) equation has produced slightly better edges compared to (Tsai, Chang and Choi, 2010) method. Even though the micro-crack pixels obtained by (Perona and Malik, 1990) equation are more complete but it also contains small but obvious contaminated pixels in the right lower part of the image as evident in Figure 7(a). However, the resulted image in Figure 7(b) proposed by (Tsai, Chang and Choi, 2010) shows there are more contaminated pixels around the borderline compared to Figure 7(a). In contrast the borderline are eliminated using (Anwar and Abdullah, 2014) ADF diffusion equation as evident from Figure 7(c). Clearly the use of multiple thresholding values as proposed by (Anwar and Abdullah, 2014) is effective in removing the background binarised pixels, leading to a more clean image. However, as clearly shown in Figure 7(c), this method leads to over filtering, causing incomplete or missing microcrack components. In contrast the proposed method produces a much more complete edges by recovering the foreground and suppressing background noise pixels. Visually, this can be seen in Figure 7(d) in which most micro-crack pixels have successfully been segmented. In addition to visual comparison, the performance of the proposed method is also evaluated numerically using the Pratt's figure of merit. The detailed is given in the following section.

### 3.3 Edge Evaluation

To evaluate the performance of proposed ADF, the Pratt's figure of merit (FOM) is employed. The details of FOM algorithm can be found in (Pratt, 1991). The mathematical FOM equation is defined as follows.

$$FOM = \frac{1}{\max(N_I, N_D)} \sum_{i=1}^{N_D} \frac{1}{1+\alpha d_i^2} \qquad (9)$$

where I9 and IJ are the number of ideal and detected edge pixels respectively. Meanwhile the symbol 5 represents a penalty constant which is used to penalise displaced edge. The default value for this parameter is set to 0 (Mehrara, Pourmohammad and Zahedinejad, 2011). Meanwhile K denotes the Euclidean distance between estimated edge point and the ideal edge pixels. In FOM analysis, a number between 0 and 1 is measured to evaluate the system performance. The value  is considered as a perfect match between ideal edge and detected pixels. In the other hand value means there is no match between predicted and detected edges. Hence, the larger the FOM the better the algorithm is. Results comparing FOMs calculated using the existing and proposed ADF methods are summarized in Table 1. Alltogether 20 different samples have been used in the comparisom. As before the parameter - used in the (Perona and Malik, 1990) and (Tsai, Chang and Choi, 2010) algorithms is rigidly fixed to 4. Meanwhile the $g$ and 4 parameters in the proposed method are obtained by using sigmoid transfer function equation as in (Anwar and Abdullah, 2014).

It can be seen from this table the average FOM of the proposed method is 0.5703, compared to 0.5489 (Perona and Malik, 1990), 0.1154 (Tsai, Chang and Choi, 2010) and 0.2391 (Anwar and Abdullah, 2014). In this case the (Tsai, Chang and Choi, 2010) and (Anwar and Abdullah, 2014) produced the lowest and second lowest FOMs respectively. Clearly both algorithms have difficulties in binarising the micro-crack pixels as visually predicted in Figure 7. Meanwhile the FOMs for (Perona and Malik, 1990) and proposed algorithms are consistently much higher compared to (Tsai, Chang and Choi, 2010) and (Anwar and Abdullah, 2014) methods.

**Table 1.** Edge evaluation performance

| No. of Samples | Image Segmentation - Double Thresholding | | | |
|---|---|---|---|---|
| | (Perona and Malik, 1990) | (Tsai, Chang and Choi, 2010) | (Anwar and Abdullah, 2014) | Proposed method |
| 1 | 0.1571 | 0.0258 | 0.0195 | 0.6078 |
| 2 | 0.2582 | 0.0525 | 0.1380 | 0.5766 |
| 3 | 0.4959 | 0.1610 | 0.3068 | 0.4575 |
| 4 | 0.6900 | 0.0627 | 0.4395 | 0.3162 |
| 5 | 0.5588 | 0.2877 | 0.5845 | 0.8014 |
| 6 | 0.4489 | 0.0425 | 0 | 0.5825 |
| 7 | 0.7259 | 0.1708 | 0.5759 | 0.8434 |
| 8 | 0.7720 | 0.0897 | 0.1458 | 0.7356 |
| 9 | 0.7813 | 0.0534 | 0.0531 | 0.6820 |
| 10 | 0.5065 | 0.0411 | 0.3874 | 0.4016 |
| 11 | 0.6077 | 0.0741 | 0.1163 | 0.6638 |
| 12 | 0.6371 | 0.1193 | 0.1234 | 0.6989 |
| 13 | 0.6782 | 0.0897 | 0.1667 | 0.6772 |
| 14 | 0.8356 | 0.0420 | 0.0243 | 0.6845 |
| 15 | 0.6675 | 0.0871 | 0.3818 | 0.8472 |
| 16 | 0.6176 | 0.3099 | 0.7721 | 0.5366 |
| 17 | 0.7662 | 0.4870 | 0.4608 | 0.6424 |
| 18 | 0.0671 | 0.0606 | 0.0690 | 0.2664 |
| 19 | 0.3401 | 0.0004 | 0.0198 | 0.1392 |
| 20 | 0.3966 | 0.0649 | 0.0331 | 0.2674 |
| Average | 0.5489 | 0.1154 | 0.2391 | 0.5703 |

In summary these results provide a convincing evidence of the superior performance of the proposed technique over others. We also realize that the sensitivity of proposed method on the choice of / and 2 parameters. These parameters, if wrongly chosen, may fail to produce satisfactory results. The future research will focus on determining the optimal values of these parameters using an iterative approach.

**Conclusions**

In this study, a new diffusion equation needed in the ADF filter is developed for enhancing the microcrack pixels on eggshell. The results are compared qualitatively and quantitatively with the original ADF version including two of its latest variants. The results indicate the important of -, / and *a* parameters in the filtering process. It was discovered that the quality of the filtered image depends critically on the choice of these parameters. In conclusion, the proposed diffusion equation outperforms other existing ADF approaches on FOM scale.

**Acknowledgements**

This work has been supported by the Universiti Sains Malaysia (USM) Research University Grant 814024.

**References**

[1] Lawrence, K. C., Yoon, S. C., Heitschmidt, G. W., Jones, D. R., Park, B., 2008. Imaging system with modified-pressure chamber for crack detection in shell eggs, *Sens. Instrum. Food Qual.* vol. 2, pp. 116–122.

[2] Yongyu, L., Sagar, D., Yankun, P., 2012. A machine vision system for identification of micro-crack in egg shell, *Journal of Food Engineering*, vol. 109, pp. 127-134.

[3] Pan, L-qing., Zhan, G., Tu, K., Tu, S., Liu, P., 2011. Eggshell crack detection based on computer vision and acoustic response by means of back-propagation artificial neural network, *European Food Research and Technology*, vol. 233, pp. 457-463.

[4] Wang, J., Jiang, R., 2005. Eggshell crack detection by dynamic frequency analysis, *European Food Research and Technology*, vol. 221, pp. 214-220.

[5] Sun, L., Bi, X-K., Lin, H., Zhao, J-W., Cai, J-R., 2013. On-line detection of eggshell crack based on acoustic resonance analysis, *Journal of Food Engineering*, vol. 116, pp. 240–245.

[6] Pan, L. Q., Tu, K.. Su, Z. P., 2007. Crack detection in eggs using computer vision and BP neural network, *Trans CSAE*, vol. 23, pp. 154–158.

[7] Perona, P., Malik, J., 1990. Scale-Space and Edge Detection Using Anisotropic Diffusion, *IEEE Trans. on Pattern Analysis and Machine Intelligence*, vol. 12.

[8] Tsai, D-M., Chang, C-C., Chao, S-M., 2010. Micro-crack inspection in heterogeneously textured solar wafers using anisotropic diffusion, *Image and Vision Computing*, vol. 28, pp. 491-501.

[9] Anwar, S. A., Abdullah, M. Z., 2014. Micro-crack detection of multicrystalline solar cells featuring an improved anisotropic diffusion filter and image segmentation technique, *EURASIP Journal on Image and Video Processing*, vol. 15, pp. 1-17.

[10] Nashat, S., Abdullah, A., Abdullah, M.Z., 2012. Unimodal thresholding for Laplacian-based Canny–Deriche filter, *Pattern Recognition Letters*, vol. 33, pp. 1269–1286.

[11] Pratt, W.K., 1991. Digital Image Processing, 2nd edition, John Wiley & Sons, New York.

[12] Mehrara, H., Pourmohammad, A., Zahedinejad, E., 2011. Nonlinear Edge Detection Based on Image Density, *Int. Journal on Recent Trends in Engineering and Technology*, vol. 6, pp. 178-183.